Korean J. Chem. Eng., **31**(7), 1253-1264 (2014)
DOI: 10.1007/s11814-014-0033-3

pISSN: 0256-1115
eISSN: 1975-7220

Experimental measurement and modeling of saturated reservoir oil viscosity

Abdolhossein Hemmati-Sarapardeh*,, Seyed-Mohammad-Javad Majidi*,***, Behnam Mahmoudi**, Ahmad Ramazani S. A.*,†, and Amir H. Mohammadi****,*****,†**

*Department of Chemical and Petroleum Engineering, Sharif University of Technology, Tehran, Iran
**Department of Petroleum Engineering, Amirkabir University of Technology, Tehran, Iran
***Department of Petroleum Engineering, Petroleum University of Technolog, Ahwaz, Iran
****Institut de Recherche en Génie Chimique et Pétrolier (IRGCP), Paris Cedex, France
*****Thermodynamics Research Unit, School of Chemical Engineering, University of KwaZulu-Natal, Howard College Campus, King George V Avenue, Durban 4041, South Africa
(*Received 5 November 2013 • accepted 27 January 2014*)

Abstract−A novel mathematical-based approach is proposed to develop reliable models for prediction of saturated crude oil viscosity in a wide range of PVT properties. A new soft computing approach, namely least square support vector machine modeling optimized with coupled simulated annealing optimization technique, is proposed. Six models have been developed to predict saturated oil viscosity, which are designed in such a way that could predict saturated oil viscosity with every available PVT parameter. The constructed models are evaluated by carrying out extensive experimental saturated crude oil viscosity data from Iranian oil reservoirs, which were measured using a "Rolling Ball viscometer." To evaluate the performance and accuracy of these models, statistical and graphical error analyses were used simultaneously. The obtained results demonstrated that the proposed models are more robust, reliable and efficient than existing techniques for prediction of saturated crude oil viscosity.

Keywords: Viscosity, Experimental Data, LSSVM, Model, Oil, Petroleum

INTRODUCTION

Viscosity as a fundamental physical property of crude oil, plays a key role in reservoir evaluation in performance calculation, reservoir simulation, forecasting production, and designing production facilities as well as planning thermal enhanced oil recovery methods [1-10]. Consequently, accurate determination of this property is necessary for petroleum industry. Generally, laboratory measurement of this property is time consuming and expensive, which makes the use of predictive models more attractive.

Oil viscosity correlations can be classified, in general, into two categories [6]. The first type is those that use oil field data which are normally available, for instance oil API gravity, reservoir temperature, saturation pressure, and solution gas-oil ratio. The second type refers to those empirical and/or semi empirical models which use some parameters that are not included in the first one, for instance, reservoir fluid composition, pour point temperature, molar mass, normal boiling point, and acentric factor as well as critical temperature [11-13]. Also, some empirical or semi-empirical correlations were developed from corresponding state equations by Teja and Rice [14], Johnson et al. [15] and Johnson [16]. Although these corresponding state correlations involve multiple computations and also use fluid composition as input variable, they could not satisfactorily estimate oil viscosity [3,6].

Models for prediction of oil viscosity are developed at three regions: under-saturated region, saturated region (below and at bubble point) as well as dead oil. Several authors confirmed that correlations for under-saturated regions are more accurate than the ones for dead oil and saturated regions [3,6,7,17,18]. This is because oil viscosity variation at under-saturated region is governed by pressure differential (pressure minus bubble point pressure), and also the solution gas-oil ratio is constant in this region [7]. Many investigations, however, demonstrated that dead oil correlations are the most inaccurate ones which are normally predicted by oil API gravity as well as temperature [3,6,7]. Furthermore, most of the saturated oil viscosity correlations introduce saturated oil viscosity as a function of both dead oil viscosity and solution gas-oil ratio, [3,19-24], while others express it as a function of dead oil viscosity and pressure [6]. In addition, to increase the accuracy of correlations at saturated region, Hemmati-Sarapardeh et al. [7], Khan et al. [25], and Labedi [26] developed two distinct correlations for viscosity of crude oil at the bubble point and below bubble point region. Table 1 illustrates the origin and ranges of data used in the aforementioned saturated oil viscosity correlations.

In our previous study [7] as well as Labedi's [26] study, for modeling viscosity of below bubble point region, the bubble point oil viscosity was involved as a new correlating parameter. Involving bubble point oil viscosity as a correlation parameter increased the accuracy of the developed correlations. In spite of their high accuracy and performance, these correlations may not be applicable in the cases where experimental data of bubble point oil viscosity is not available. Moreover, almost all correlations for saturated region use dead oil viscosity as the main correlating parameter, which should be

†To whom correspondence should be addressed.
E-mail: ramazani@sharif.edu,
a.h.m@irgcp.fr, amir_h_mohammadi@yahoo.com

Table 1. The origin and PVT data ranges used in saturated oil viscosity correlations [7]

Author	Source of data	Solution GOR, SCF/STB	Saturation pressure, psia	μ_{od}, cp
Chew and connally [50](1)	US	51-3544	132-5645	0.370-50
Chew and connally [50](2)	US	51-3544	132-5645	0.370-50
Chew and connally [50](3)	US	51-3544	132-5645	0.370-50
Beggs and Robinson [20]	-	20-2070	132-5265	-
Al-Khafaji et al. [52]	-	0-2100	-	-
Khan et al. [59]	Saudi Arabia	24-1901	107-4315	0.130-77.4
Petrosky [53]	Gulf of Mexico	21-1855	1574-9552	0.210-7.4
Labedi [26]	Libya	13-3533	60-6358	0.115-3.72
Kartoatmodjo and Schmidt [58]	Worldwide	2.3-572	15-6054	0.100-6.3
Elsharkawy and Alikhan [3]	Middle East	10-3600	100-3700	0.050-21
Hossain et al. [54]	Worldwide	19-493	121-6272	3.600-360
Naseri et al. [6]	Iran	255-4116	420-5900	0.110-18.15
Bergman and Sutton [24]	Worldwide	6-6525	66-10300	0.210-4277

determined through laboratory analysis. When experimental data of dead oil viscosity is not available, it is predicted by correlations that are not satisfactorily accurate, subsequently leading into inaccurate prediction of crude oil viscosity at saturated region. Unfortunately, the developed models in the saturated region are not accuare enough even when experimental dead oil viscosity is available [3,6].

The present study aims to solve the already mentioned problems associated with oil viscosity prediction in the saturated region. For this end, a rolling ball viscometer (Ruska, series 1602) was utilized to measure reservoir oil viscosity at various saturated pressures. Afterward, based on a large data bank (859 data set), covering a wide range of crude oil properties and reservoir conditions, six different models that can predict saturated oil viscosity with various input parameters have been proposed. The proposed strategy utilizes least square support vector machine (LSSVM) [27] to construct nonlinear modeling. In addition, a novel feature selection mechanism based on the coupled simulated annealing (CSA) optimization for tuning the optimal parameters has been proposed. CSA-LSSVM models are adequate candidates for characterizing the nonlinear behavior. Additionally, statistical and graphical error analyses are carried out to establish the adequacy and accuracy of these six models as well as existing correlations. The obtained results demonstrate that the developed models provide predictions in satisfactory agreement with the experimental data and outperform all of the previously published ones. These CSA-LSSVM models can be implemented in any reservoir simulator software and provide better accuracy and performance over the existing methods.

EXPERIMENTAL EQUIPMENT AND PROCEDURE

We used a rolling ball viscometer (Ruska, series 1602) to measure reservoir oil viscosity at various saturated pressures. Although this instrument has some limitations for heavy oil, it is especially suitable for black and volatile oil. Before beginning the measurements, it is necessary to calibrate this instrument with a known viscosity standard liquid similar to the fluid to be measured. The instrument consists of a highly polished stainless steel barrel, which can be closed at the top by means of a plunger. A steel ball rolls within the barrel, its diameter being to some extent smaller than the bore, and the barrel is filled entirely with the fluid to be studied. The barrel is inclined at a certain angle and the ball rolls along it under gravity for a measured distance. The roll time is determined by a digital timer. In fact, the roll time interval is a measure of the viscosity. If the clearance between the bore of the barrel and the ball diameter is excessively small, then the flow of fluid will be turbulent. Under these conditions the Rolling Ball instrument does not measure viscosity correctly because the theory assumes laminar flow. To control the rolling time, measurements can be made at different angles or the stainless steel ball and/or the barrel may be replaced with a different diameter. The governing equation is as follows:

$$\mu_o = A(\rho_{ball} - \rho_{oil})t + B \quad (1)$$

where μ_o represents oil viscosity, t is rolling time in seconds, ($\rho_{ball} - \rho_{oil}$) denotes difference in density between ball and oil and A & B are constants of the system determined from calibration with fluid of known viscosity.

Oil viscosities are normally measured at reservoir temperature over a range of pressures both above and below the bubble point pressure extending down to near atmospheric pressure. Measurements below bubble point pressure are made under differential conditions, *i.e.*, matched as closely as possible to the stage pressures used for the differential vaporization. Rolling Ball viscometers are constructed in such a way that allows a pseudo differential vaporization of gas to be conducted within them, leaving the oil to fill the measuring chamber. In this way, the viscosity of the oil in the reservoir can be measured as gas is depleted from it. The change in viscosity with release of gas is normally very large [7].

Table 2. The data ranges and their corresponding statistical parameters used in this study

Inputs	Min	Max	Average	Standard deviation
API	13.35	44.83	27.23	6.15
T, °F	110	290	218.41	41.42
R_s, SCF/STB	0	2512.67	425.50	383.70
P, psi	14.7	5294.8	1310.4	1089.9
μ_o, cp	0.17	37.18	1.68	2.04

In the present work, a large database including PVT experimental data of 859 series of Iranian oil reservoirs has been measured to develop novel CSA-LSSVM models, as pointed out earlier. Note that more than 400 data sets of these large databases have been previously used in developing oil viscosity correlations for bubble point and below bubble point region [7]. These data include oil API gravity, reservoir temperature, pressure, bubble point pressure, and solution gas-oil ratio as well as PVT measurements (oil characterization) at reservoir temperature. The ranges of these data cover almost all Iranian oil reservoirs PVT, data and subsequently the developed models based on these data could be reliable for prediction of other Iranian oil reservoirs viscosity, as mentioned earlier. Table 2 summarizes

Table 3. Experimental oil viscosity data and their corresponding PVT properties*

P, psi	Rs, SCF/STB	μ_o, cp	P, psi	Rs, SCF/STB	μ_o, cp
Sample 1			Sample 2		
μ_{od}=3.33, μ_{ob}=1.56, P_b=909.1, T=204, API=13.35			μ_{od}=6.33, μ_{ob}=3.18, P_b=391.0, T=208, API=21.85		
909.1	131.18	1.56	391.0	157.99	3.18
623.0	98.71	1.90	319.0	147.38	3.33
423.0	76.68	2.12	217.0	127.20	3.58
223.0	51.42	2.53	115.0	89.76	3.82
14.7	0.00	3.33	14.7	0.00	6.33
Sample 3			Sample 4		
μ_{od}=16.71, μ_{ob}=3.88, P_b=2205.0, T=205, API=17.3			μ_{od}=8.61, μ_{ob}=6.04, P_b=2144.1, T=198, API=18.31		
2205.0	492.91	3.88	2144.0	463.01	6.05
1800.0	422.71	4.10	1835.0	408.62	6.19
1502.0	371.24	4.29	1535.0	358.01	6.31
1204.0	320.34	4.68	1235.0	306.69	6.40
905.0	266.20	5.21	928.0	254.24	6.64
605.0	210.66	5.93	420.0	161.45	7.46
305.0	146.71	7.20	217.0	103.30	7.97
14.7	0.00	16.71	14.7	0.00	8.61
Sample 5			Sample 6		
μ_{od}=37.18, μ_{ob}=18.16, P_b=730.0, T=132, API=18.55			μ_{od}=5.07, μ_{ob}=1.88, P_b=1668.0, T=220, API=18.69		
729.8	126.11	18.16	1668.3	389.91	1.89
605.0	111.78	18.90	1236.0	309.56	2.01
455.0	92.90	19.96	935.0	256.87	2.14
305.0	71.41	22.18	632.0	201.52	2.33
158.0	47.75	25.58	329.0	139.52	2.69
14.7	0.00	37.18	14.7	0.00	5.07
Sample 7			Sample 8		
μ_{od}=7.78, μ_{ob}=1.87, P_b=2390.0, T=238, API=17.98			μ_{od}=7.52, μ_{ob}=2.05, P_b=2461.0, T=238, API=19.17		
2390.0	568.58	1.87	2461.0	576.63	2.05
1933.0	475.82	1.99	2033.0	490.31	2.12
1533.0	398.58	2.24	1633.0	412.53	2.26
1133.0	321.92	2.54	1233.0	334.39	2.45
733.0	243.91	3.05	833.0	258.95	2.83
333.0	146.16	3.80	433.0	166.63	3.52
14.7	0.00	7.78	14.7	0.00	7.52
Sample 9			Sample 10		
μ_{od}=1.70, μ_{ob}=0.72, P_b=4966.0, T=229, API=31.3			μ_{od}=12.13, μ_{ob}=3.50, P_b=1607.3, T=205, API=19.6		
4966.0	1910.09	0.72	1607.3	377.78	3.51
4033.0	1568.89	0.80	1254.0	317.93	3.73
3033.0	1126.88	0.86	1005.0	274.22	3.96
2033.0	643.99	0.92	755.0	229.88	4.28
1033.0	371.99	1.07	505.0	182.78	4.75
533.0	234.80	1.24	255.0	126.99	5.68
14.7	0.00	1.70	14.7	0.00	12.13

these study data ranges as well as their corresponding statistical parameters. More than 120 data sets of experimental oil viscosities and their corresponding PVT properties are reported in Table 3. More detailed information is available upon request.

MODEL DEVELOPMENT

1. Model Parameters Selection

As previously mentioned, saturated oil viscosity is predicted by

Table 3. Continued

P, psi	Rs, SCF/STB	μ_o, cp	P, psi	Rs, SCF/STB	μ_o, cp
Sample 11			Sample 12		
μ_{od}=4.28, μ_{ob}=2.38, P_b=1685.0, T=236, API=19.76			μ_{od}=5.67, μ_{ob}=1.91, Pμ=1670.0, T=236, API=19.83		
1685.0	421.13	2.38	1670.0	388.46	1.91
1503.0	386.29	2.43	1254.0	315.18	2.01
1205.0	331.77	2.63	1005.0	271.44	2.21
905.0	275.45	2.85	755.0	227.32	2.47
605.0	216.92	3.14	505.0	179.75	2.87
305.0	147.93	3.61	255.0	123.63	3.35
14.7	0.00	4.28	14.7	0.00	5.67
Sample 13			Sample 14		
μ_{od}=10.81, μ_{ob}=3.98, P_b=1071.0, T=205, API=19.94			μ_{od}=7.26, μ_{ob}=2.57, P_b=1379.4, T=222, API=20.11		
1071.4	289.30	3.98	1379.4	339.37	2.57
805.0	249.00	4.07	1220.0	311.70	2.58
605.0	212.23	4.34	918.0	258.00	2.63
405.0	171.65	4.66	618.0	202.60	2.80
205.0	121.98	5.32	318.0	139.39	3.40
14.7	0.00	10.81	14.7	0.00	7.26
Sample 15			Sample 16		
μ_{od}=10.07, μ_{ob}=3.86, P_b=1090.0, T=205, API=20.14			μ_{od}=5.65, μ_{ob}=2.04, P_b=1722.0, T=255, API=20.17		
1089.8	292.09	3.87	1722.0	449.99	2.04
905.0	265.22	3.95	1231.0	357.52	2.23
705.0	227.44	4.15	928.0	298.24	2.36
505.0	189.10	4.50	623.0	236.13	2.64
255.0	137.46	5.20	319.0	164.65	3.09
14.7	0.00	10.08	14.7	0.00	5.65
Sample 17			Sample 18		
μ_{od}=1.88, μ_{ob}=0.44, P_b=3528.0, T=235, API=31.06			μ_{od}=1.28, μ_{ob}=0.30, P_b=4301.5, T=239, API=31.25		
3527.6	1051.47	0.44	4301.5	1588.99	0.30
2989.0	883.81	0.47	3591.0	1226.24	0.34
2489.0	734.89	0.51	2978.0	955.99	0.37
1989.0	600.52	0.56	2393.0	767.77	0.42
1490.0	476.44	0.63	1800.0	594.89	0.49
990.0	357.71	0.74	1204.0	436.71	0.60
490.0	236.02	0.98	605.0	278.56	0.77
14.7	0.00	1.88	14.7	0.00	1.28
Sample 19			Sample 20		
μ_{od}=3.60, μ_{ob}=1.62, P_b=2400.0, T=150, API=31.51			μ_{od}=3.26, μ_{ob}=1.28, P_b=2387.4, T=150, API=31.51		
2400.0	699.20	1.62	2387.4	706.39	1.28
1939.0	580.55	1.64	2040.0	616.04	1.32
1333.0	434.24	1.69	1636.0	514.32	1.38
929.0	336.15	1.79	1231.0	415.46	1.50
629.0	268.17	1.91	826.0	317.44	1.69
420.0	210.43	2.10	420.0	213.20	1.96
14.7	0.00	3.60	14.7	0.00	3.26

*More information regarding these reservoir fluids is available upon request to the authors

Table 4. The input parameters to each model developed in this study

Model	Input
Model 1	T, API, P
Model 2	T, API, Rs
Model 3	P, μ_{od}
Model 4	μ_{od}, P, P_b
Model 5	Rs, μ_{od}
Model 6	Rs, P, P_b, μ_{ob}, μ_{od}

various properties such as dead oil viscosity, solution gas-oil ratio, pressure, bubble point pressure, and bubble point viscosity. Mostly, because experimental data of dead oil viscosity is not available, dead oil viscosity is also predicted by correlations, and subsequently this inaccurate prediction leads to inaccurate results for saturated oil viscosity. We developed six different models based on LSSVM strategy. The first two models use temperature and oil API gravity as correlating parameters instead of dead oil viscosity. In addition, three models similar to most of previously published correlations have been proposed in which saturated oil viscosity is related to dead oil viscosity and some other properties such as pressure, bubble point pressure, and solution gas-oil ratio. Finally, the last model was developed based on dead oil viscosity, bubble point oil viscosity, pressure, and bubble point pressure as well as solution gas-oil ratio. These models are designed in such a way that can predict saturated oil viscosity by every available PVT parameter. The input parameters of each model are illustrated in Table 4.

2. Characteristics of the Support Vector Machine

This study aims to develop nonlinear relationships among the available experimental data considered as inputs of the model and their corresponding output. To find such a model, an appropriate mathematical tool is required. The support vector machine (SVM) is a robust and powerful methodology developed from the machine-learning community [27-29]. SVM is a tool for a set of related supervised learning methods which analyze data and recognize patterns and are used for regression analysis. The SVM is considered as a non-probabilistic binary linear classifier. Some of the advantages of SVM-based models over the common artificial nal networks (ANNs) models are as below [27,28].

They are more likely to converge to the global optima. In addition, prior determination of the network topology is not required in these models and can be automatically determined as the training process ends. Moreover, the number of hidden nodes and hidden layers should not be determined. These methods have also fewer adjustable parameters (typically two) compared to ANN methods. Also, they normally result in a solution that can be quickly obtained by a standard algorithm (quadratic programming). Over-fitting problems are less probable in SVM method and also they have proper generalization performance. More details about ANN models and algorithmic differences between SVM and ANNs can be found elsewhere [30,31].

Suykens and Vandewalle [27] modified the original SVM to support the solution of the original SVM algorithm set of nonlinear equations (quadratic programming). The consequent least-squares SVM (LSSVM) [27] methodology benefits from advantages like those of SVM although it only requires solving a set of linear equations (linear programming), resulting in a faster and more appropriate alternative to the traditional SVM strategy.

3. Data Normalization

During training of the LSSVM, higher valued input variables may tend to suppress the influence of the smaller ones. To overcome such a problem and to make LSSVM perform appropriately, data must be well processed and adequately scaled before input to the LSSVM. All the inputs and their corresponding outputs were normalized using the following equation:

$$x_n = \left(\frac{x}{1.5 \times x_{max}}\right) \times 0.8 + 0.1 \tag{2}$$

where, x is actual data, x_{max} shows the maximum value of the data and x_n denotes the normalized data [32]. Normalization procedure, which is generally used in an optimization process, has been employed to obtain the parameters of LSSVM algorithm, and it has no effect on the model results [33-35]. At the end, these values were changed to their original values.

4. Equations

The regression error of the LSSVM strategy is determined as the difference between the represented and predicted property values and experimental ones, which is considered as an addition to the optimization problem constraint. In most commonly used SVM approaches, the value of the regression error is normally optimized during the calculations, while in the LSSVM, it is mathematically defined [27,28,36,37].

The penalized cost function of the applied approach is defined as below [38,39]:

$$Q_{LSSVM} = \frac{1}{2} w^T w + \gamma \sum_{k=1}^{N} e_k^2 \tag{3}$$

Exposed to the following constraint:

$$y_k = w^T \varphi(x_k) + b + e_k \quad k = 1, 2 \ldots N \tag{4}$$

where x is the input vector of the model parameters, y expresses the outputs, b shows the intercept of the linear regression in the modified SVM method (LSSVM), w displays the regression weight (slope of the linear regression), e_k stands for the regression error for N training objects (the least-squares error approach), γ exhibits the relative weight of the summation of the regression errors compared to the regression weight (first right hand side of Eq. (4)), φ denotes the feature map, in which the experimental data can be linearly separated by a hyperplane specified by the pair ($w \in R^m$, $b \in R$), and superscript T stands for the transpose matrix [27,28,36,38,39].

The weight coefficient (w) is normally written as follows:

$$w = \sum_{k=1}^{N} \alpha_k x_k \tag{5}$$

Where,

$$\alpha_k = 2\gamma e_k \tag{6}$$

Eq. (4) is re-arranged as follows, using the principles of the LSSVM approach [27,28,35,36]:

$$y = \sum_{k=1}^{N} \alpha_k x_k^T x + b \tag{7}$$

Thus, the Lagrange multipliers (α_k) are calculated as [27,28,35,36]:

$$\alpha_k = \frac{(y_k - b)}{x_k^T x + (2\gamma)^{-1}} \quad (8)$$

The aforementioned linear regression equation could be re-treated as a nonlinear one using the Kernel function as follows [27,28,35]:

$$f(x) = \sum_{k=1}^{N} \alpha_k K(x, x_k) + b \quad (9)$$

where $K(x, x_k)$ is the Kernel function calculated from the inner product of the two vectors x and x_k in the feasible region built by the inner product of the vectors $\Phi(x)$ and $\Phi(x_k)$ as follows:

$$K(x, x_k) = \Phi(x)^T . \Phi(x_k) \quad (10)$$

In this work, the radial basis function (RBF) Kernel has been utilized as below [27,28,35,38,39]:

$$K(x, x_k) = \exp(-\|x_k - x\|^2 / \sigma^2) \quad (11)$$

where σ is a decision variable, which is optimized through an external optimization algorithm during the calculations. The mean square error (MSE) of the results of the LSSVM algorithm has been evaluated using the following equation:

$$MSE = \frac{\sum_{i=1}^{n} (\mu_{o_{rep./pred.}} - \mu_{o_{exp.}})^2}{n} \quad (12)$$

where μ_o is the oil viscosity, subscripts rep./pred. and exp. stand for the represented/predicted, and experimental oil viscosity, respectively, and n denotes the number of samples from the initial population. In this study, the LSSVM algorithm developed by Pelckmans et al. [34] and Suykenes and Vanewalle [27] has been used.

5. Coupled Simulated Annealing

Simulated annealing (SA) [40-43] is said to be the earliest algorithm extending local search methods with an explicit algorithm to escape from local optima. The principal idea is to allow moves that result in solutions of worse quality than the current solution to facilitate escaping from local optima. The probability of doing such a move is decreased during the search process. CSA is a modified version of SA that is designed to be able to easily escape from local optima and consequently improve the accuracy of solutions without slowing down too much the speed of convergence. Suykens and Vandewalle [44] presented original principles of this method and showed that coupling among local optimization processes can be utilized to improve gradient optimization methods to escape from local optima in non-convex problems. Moreover, with the aim of increasing the quality of the final solution, Xavier-de-Souza et al. [45] demonstrated the use of coupling in a global optimization method. In addition, by designing a coupling strategy with minimal communication, these coupled methods can be employed very efficiently in parallel computer architectures, making them very attractive to the multi-core trend in the new generation of computer architectures [46]. More details about this algorithm can be found elsewhere [47].

6. Computational Procedure

In this part of our study, the database is randomly divided into two sub data sets consisting of the "training" set and the "test" set. Normally, the "training" set is applied to generate the model structure, and the "test (prediction)" set is employed to investigate its prediction capability and validity. To pursue our objective, 80% of

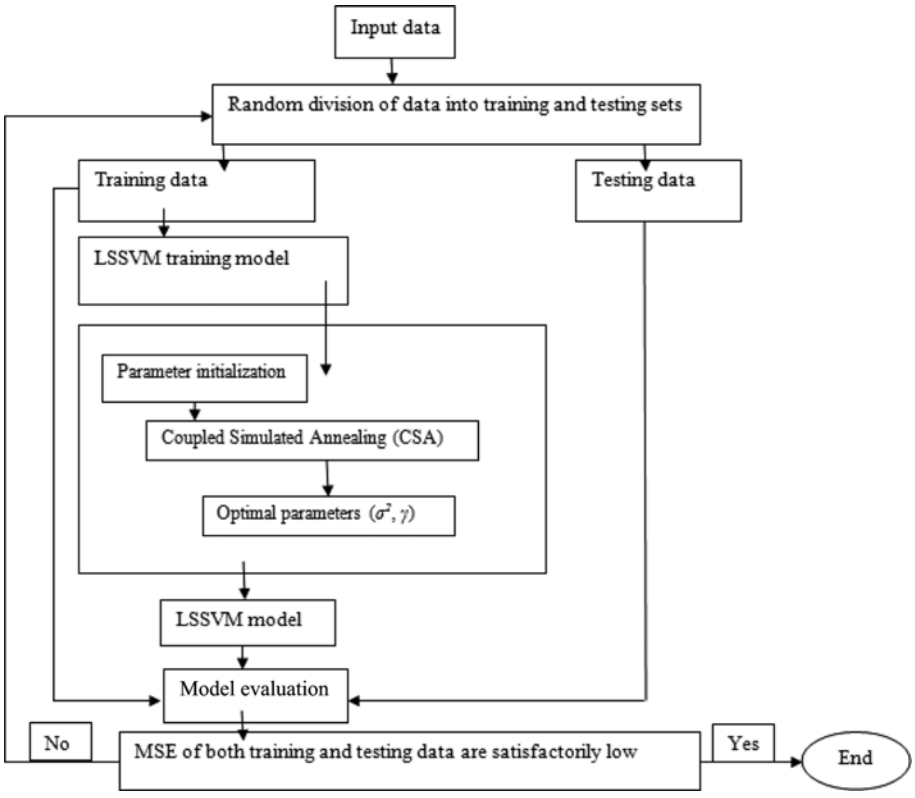

Fig. 1. The flow chart of the CSA-LSSVM model used for modeling saturated oil viscosity.

the main data set randomly selected for the "training" set and the remaining 20% has been considered as the "testing (prediction)" set. In distribution of the data into these two sub data sets, in general, many distributions have been employed to avoid the local accumulations of the data in the feasible region of the problem. Consequently, the satisfactory distribution is the one with homogeneous accumulations of the data on the domain of the two sub data sets. The flow chart for the algorithm used in this study is shown in Fig. 1.

PERFORMANCE EVALUATION

1. Statistical Error Analysis

To determine the accuracy and performance of the proposed model several statistical parameters have been employed consisting of average percent relative error, average percent absolute relative error, standard deviation of error, root mean square error and coefficient of determination [7,43,48]. Definitions and equations of those parameters are given below.

1. Average percent relative error (APRE). It measures the relative deviation from the experimental data, defined by:

$$E_r\% = \frac{1}{n}\sum_{i=1}^{n} E_i\% \tag{13}$$

where $E_i\%$ is the relative deviation of a represented/predicted value from an experimental value and is expressed as percent relative error:

$$E_i\% = \left[\frac{(\mu_o)_{exp} - (\mu_o)_{rep./pred}}{(\mu_o)_{exp}}\right] \times 100 \Rightarrow i = 1,2,3,\ldots,n \tag{14}$$

2. Average absolute percent relative error (AAPRE). It evaluates the relative absolute deviation from the experimental data, defined as below:

$$E_a\% = \frac{1}{n}\sum_{i=1}^{n} |E_i\%| \tag{15}$$

3. Root mean square error (RMSE). It measures the data scattering around zero deviation, defined by:

$$RMSE = \sqrt{\frac{1}{n}\sum_{i=1}^{n} (\mu_{oi_{exp}} - \mu_{oi_{rep./pred}})^2} \tag{16}$$

4. Standard deviation (SD). It is a measure of dispersion and a lower value of it shows a smaller degree of scatter. It is defined as:

$$SD = \sqrt{\frac{1}{n-1}\sum_{i=1}^{n} \left(\frac{\mu_{oi_{exp}} - \mu_{oi_{rep./pred}}}{\mu_{oi_{exp}}}\right)^2} \tag{17}$$

5. Coefficient of determination (R^2). It is a simple statistical parameter that reveals how good the model matches the data and, as a result, represents a measure of the utility of the model. As a matter of fact, the closer the value of R^2 to 1, the better the model fits the data. It is defined as:

$$R^2 = 1 - \frac{\sum_{i=1}^{n} (\mu_{oi_{exp}} - \mu_{oi_{rep./pred}})^2}{\sum_{i=1}^{n} (\mu_{oi_{rep./pred}} - \overline{\mu_o})^2} \tag{18}$$

where $\overline{\mu_o}$ is the mean of the experimental data values as presented in the above formula.

2. Graphical Error Analysis

To visualize the accuracy and performance of a model, generally, two graphical analyses are employed in which crossplot and error distribution curves are sketched [7,43,48].

1. Error distribution: It is a strategy to measure error distribution around the zero error line to illustrate if the model has an error trend or not.

2. Crossplots: In this technique, all represented/predicted values are sketched against the experimental values and therefore a crossplot is created. A 45° straight line (unit slope line) between the experimental values and represented/predicted data points on the crossplot, shows the perfect model line. The closer the plotted data to the 45° perfect model line, the higher is the consistency of the model.

RESULTS AND DISCUSSION

As it is known, viscosity of crude oil is influenced by oil API gravity, solution gas-oil ratio, pressure, and temperature. In this work, all the experiments were performed at reservoir temperature. Solution gas-oil ratio at pressures above bubble point pressure is constant and the oil viscosity in this region is governed by pressure differential (pressure minus bubble point pressure). However, starting

Table 5. Statistical error analysis for correlation calculating saturated oil viscosity

Author	E_a (%)	E_r (%)	R^2	RMSE	SD
Chew and Connally [50][1]	19.04	−3.00	0.2065	0.70	0.24
Chew and Connally [50][2]	27.37	6.34	0.2247	0.99	0.33
Chew and Connally [50][3]	18.53	1.66	0.2031	0.62	0.31
Beggs and Robinson [20]	27.00	25.55	0.1807	1.04	0.31
Al-Khafaji et al. [52]	16.78	3.54	0.9315	0.61	0.22
Khan et al. [59]	22.24	−21.64	0.2372	0.69	0.32
Petrosky [53]	18.24	11.47	0.9305	0.71	0.23
Labedi [26]	8.13	−1.73	0.2351	0.38	0.13
Kartoatmodjo and Schmidt [58]	20.01	10.89	0.9283	0.64	0.18
Elsharkawy and Alikhan [3]	19.22	14.09	0.9313	0.79	0.24
Hossain et al. [54]	259.75	−247.00	0.0020	23.23	32.97
Naseri et al. [6]	34.90	31.72	0.8805	0.98	0.39
Bergman and Sutton [24]	19.11	15.12	0.9311	0.72	0.24

from bubble point pressure, solution gas-oil ratio decreases with reduction in pressure until dead oil in which all gases release from the crude oil. To evaluate the capability and accuracy of the existing correlations for saturated crude oil viscosity, a large database covering a wide range of conditions from Iranian oil reservoirs have been utilized. Statistical error analysis, which is reported in Table 5, has been employed to establish the performance of these correlations. Input parameters of these correlations are mostly dead oil viscosity and solution gas-oil ratio. In this research, the experimental dead oil viscosity, which is a correlating parameter for saturated oil viscosity, has been used in the aforementioned correlations. The obtained results indicated inaccuracy of these correlations for prediction of saturated crude oil viscosity. As can be seen, the Labedi [26] correlation shows more accurate results compared to the other ones. It is because this correlation utilizes bubble point viscosity as correlating parameter which is rarely present in PVT experimental reports. This correlation may not be applicable in any reservoir simulator for prediction of saturated oil viscosity. However, employing experimental dead oil viscosity and bubble oil viscosity data could strongly improve efficiency and robustness of models for prediction of saturated oil viscosity [7]. Moreover, it can be concluded from Table 5 that the Khan et al. [25] correlation and Hossain et al. [23] correlation overstimate saturated oil viscosity, while the correlations of Beggs and Robinson [20], Elsharkawy and Alikhan [3], Naseri et al. [6], and Bergman and Sutton [24] understimate this property. In addition, Hossain et al. [23] is the worst predictive model for saturated viscosity because this correlation was developed only for heavy oils. The obtained results in this study are consistent and in good agreement with previously published investigations [7].

In the next step, to solve associated problems with prediction of saturated oil viscosity, six CSA-LSSVM models have been designed in such a way that could predict saturated oil viscosity with every available PVT data. For this end, model 1 and model 2 are constructed to predict saturated oil viscosity whenever the experimental dead oil viscosity is unavailable. In contrast to previously published saturated oil viscosity correlations, which first calculate dead oil viscosity from empirical correlations whenever experimental dead oil viscosity data are not available and then predict saturated oil viscosity, models 1 and 2 directly predict saturated oil viscosity with one step calculations. It has been proven that dead oil viscosity correlations are not satisfactorily accurate [3,6], and it subsequently leads to tremendous unreliable prediction of saturated oil viscosity. Both models 1 and 2 use three correlating parameters. The two first input parameters of Models 1 and 2 are oil API gravity, temperature, and the third correlating parameter in model 1 is pressure, while solution gas-oil ratio was designed as the last correlating parameter in model 2. In addition to these two models, three models similar to most of the literature correlations have been deigned to predict saturated oil viscosity as a function of dead oil viscosity as well as other correlating parameters such as pressure, bubble point pressure, and solution gas-oil ratio. The first input parameter of models 3, 4 and 5 is dead oil viscosity and the second correlating parameters are pressure for model 3, pressure and bubble point pressure for model 4, and solution gas-oil ratio for model 5. Finally, model 6 was designed, in which dead oil viscosity, bubble point viscosity, pressure, bubble point pressure, and solution gas-oil ratio are required as model inputs.

Table 6. Statistical error analysis of the proposed models

Model	E_a (%)	E_r (%)	R^2	RMSE	SD
Model 1-training data	17.92	−5.68	0.8513	0.96	0.27
Model 1-test data	19.02	−7.45	0.8718	1.29	0.28
Model 2-training data	14.33	−4.20	0.9070	0.89	0.24
Model 2-test data	18.57	−5.90	0.7707	1.01	0.25
Model 3-training data	13.78	−3.08	0.9680	0.51	0.22
Model 3-test data	12.97	−1.67	0.9581	0.57	0.21
Model 4-training data	11.42	−2.27	0.9840	0.35	0.18
Model 4-test data	12.09	0.78	0.9679	0.58	0.18
Model 5-training data	12.21	−2.75	0.9754	0.45	0.17
Model 5-test data	10.94	−1.88	0.9706	0.46	0.17
Model 6-training data	1.99	−0.08	0.9997	0.05	0.03
Model 6-test data	3.66	0.61	0.9960	0.18	0.06

Table 7. The optimized parameters of LSSVM models

Model	σ^2	γ
Model 1	1.5488	901.1803
Model 2	0.4743	106.2041
Model 3	2.7479	9092.3646
Model 4	1.9546	85543.6030
Model 5	4.2840	1034548.7144
Model 6	6.7142	1823839.7401

The optimum values of the LSSVM parameters including γ and σ^2 have been optimized using CSA, as previously mentioned. The optimized values of LSSVM models are reported in Table 7. The numbers of reported digits of the above-mentioned parameters are generally obtained through sensitivity analysis of the overall error of the optimization procedure [49].

To pursue our objective, statistical error analysis in which average percent relative error, average absolute percent relative error, standard deviation of error, root mean square error and coefficient of determination are employed, and graphical error analysis in which crossplot and error distribution curves are sketched, have been utilized. Several conclusions could be drawn from Table 6: models 1 and 2 are satisfactorily accurate although they do not use experimental oil viscosity as correlating parameters. Besides, models 1 and 2 have approximately the same accuracy because at pressures below the bubble point pressure a linear relationship exists between pressure and solution gas-oil ratio.

Another conclusion which could be extracted from Table 6 is that models 3, 4 and 5, which use experimental oil viscosity, could be more robust and accurate than models 1and 2. In addition, the superiority of these three models over other correlations which use experimental dead oil viscosity as their correlating parameters is revealed (See Tables 5 and 6). Also, the results showed that model 4, which employs bubble point pressure in addition to pressure as input parameter, has not remarkable superiority over model 3 which only uses pressure and dead oil viscosity as input parameters. Moreover, comparison between models 3, 4 and 5 demonstrates that the results of model 5, which are a function of solution gas-oil ratio, are in better agreement with experimental data. It indicated the key

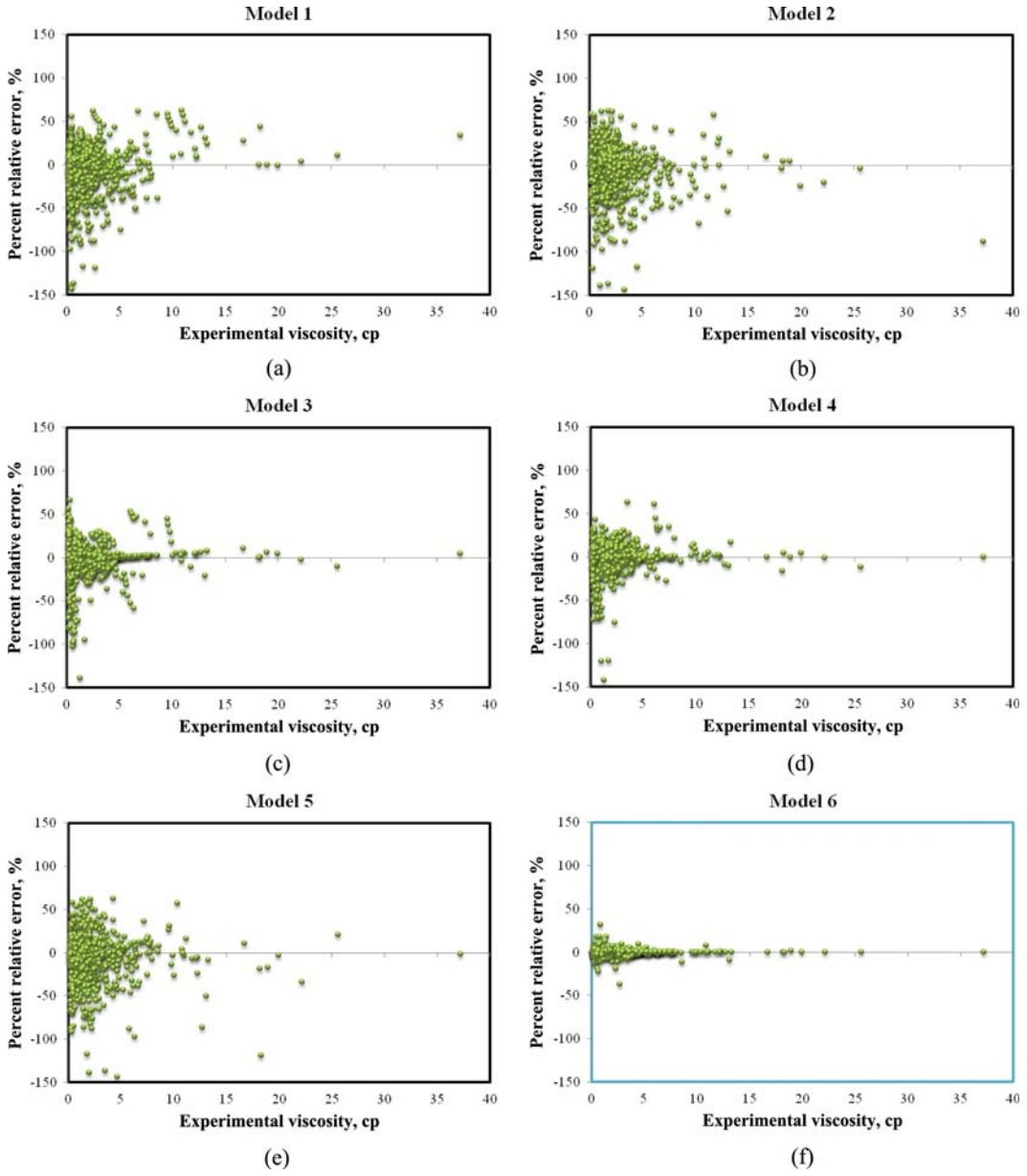

Fig. 2. Percent relative error distribution for saturated oil viscosity models.

role of solution gas-oil ratio in saturated oil viscosity. It should be noted that most of the saturated oil viscosity correlations in the literature introduce saturated oil viscosity as a function of solution gas-oil ratio rather than pressure [3,24,50-54].

Since the experimental data of bubble point oil viscosity is rarely available, model 6 may not be applicable in many petroleum industrial problems. However, this model is developed in the cases which need higher accuracy of saturated oil viscosity. It is advised to experimentally measure bubble point viscosity in order to strongly improve the accuracy of saturated oil viscosity prediction. As a matter of fact, bubble point oil viscosity is the main correlating parameter for prediction of under-saturated oil viscosity [3,7,26,53-62]. Therefore, experimental bubble point oil viscosity is required for obtaining more robust and accurate results in under-saturated region. Table 6 shows that model 6 is more effective and accurate than other developed models in this study as the well as existing correlations.

Graphical error analysis including crossplot and error distribution curve was performed to visualize the accuracy and adequacy of the developed models in this study. Fortunately, none of the developed models showed error trend or anomalous behaviors over the full range of saturated oil viscosity data (See Figs. 2(a)-(f) and 3(a)-(f)). As expected, models 1 and 2 have the lowest accuracy while models 3, 4 and 5 are more robust and accurate (Figs. 2(a)-(e) and 3(a)-(e)). In addition, models 3, 4, and 5 have a smaller error range and show lower scatter around the zero error line when compared with models 1 and 2 (Fig. 2(a)-(e)). Model 6 is the most accurate and robust model and has the smallest error range and the lowest scatter around the zero error line (See Figs. 2(f) and 3(f)). Surprisingly, all the data points lay on the unit slope line which confirms the perfect accuracy of model 6 (Fig. 3(f)).

Starting from bubble point pressure, solution gas-oil ratio decreases with reduction in pressure until dead oil in which all gases release

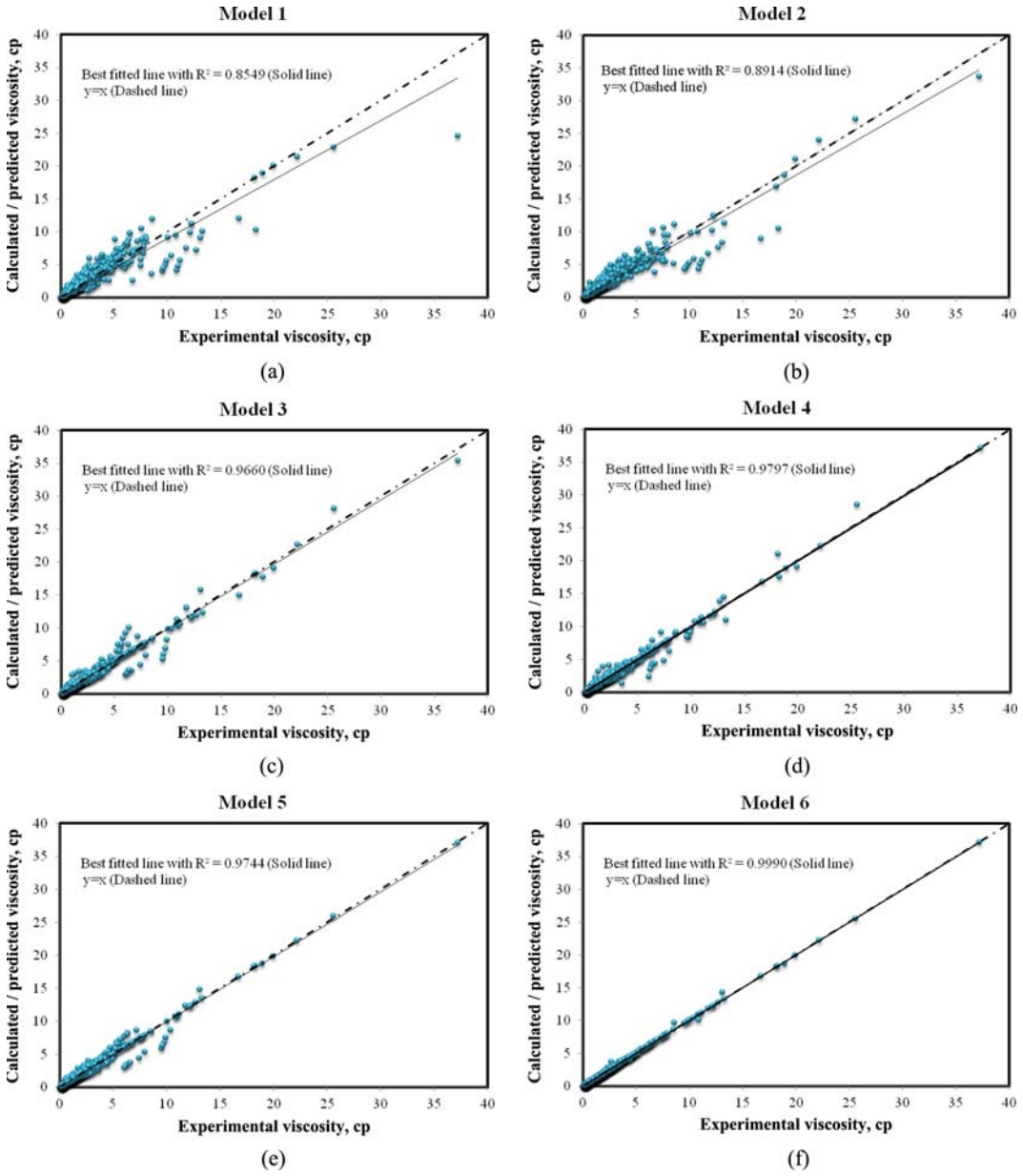

Fig. 3. Crossplots for saturated oil viscosity models.

from the crude oil, as pointed out earlier. To check the validity of the developed models in this study, one sample of Iranian oil reservoirs was selected and the experimental data as well as their corresponding predicted values by the newly developed models were sketched on the same figure (see Fig. 4). Fortunately, all the models could capture the expected trend and models 3, 4 and 5 predict saturated oil viscosities with exceptional accuracy and predicted values by model 6 fit almost all the experimental data (see Fig. 4).

CONCLUSION

A large database, including 859 data sets of saturated oil viscosity of Iranian oil reservoirs, has been measured using a rolling ball viscometer (Ruska, series 1602). Then, thirteen empirical correlations were evaluated through statistical error analyses. The results show inaccuracy of these correlations for prediction of saturated oil viscosity. The Labedi [26] correlation shows more accurate results because it uses bubble point oil viscosity as a correlating parameter, which is rarely available. It was found that the Khan et al. [59] correlation and Hossain et al. [54] correlation overstimate saturated oil viscosity, while the correlations of Beggs and Robinson [51], Elsharkawy and Alikhan [3], Bergman and Sutton [63], and Naseri et al. [6] understimate this property.

Finally, six CSA-LSSVM models have been developed which solved the associated drawbacks of previously published correlations. These CSA-LSSVM models were designed in such a way that can predict saturated oil viscosity with every available PVT experimental data. Accuracy and validation of these models have been evaluated using statistical and graphical error analyses, which indicated the superiority of these models over the existing correlations.

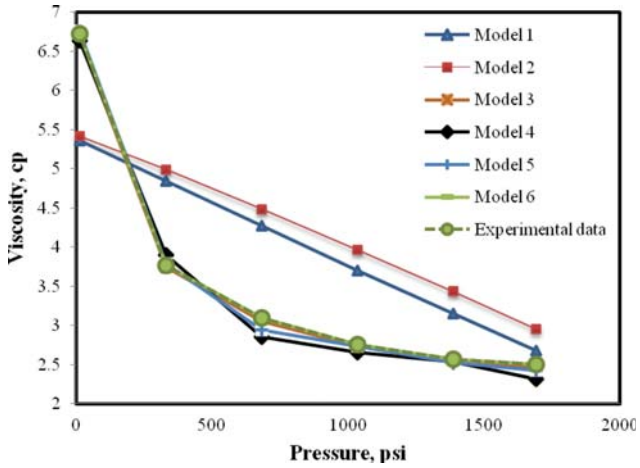

Fig. 4. Experimental data and their predicted corresponding values by newly proposed models of one saturated oil viscosity sample.

However, when applying these models, the limitations of parameters which these models have been derived from should be regarded. These new models can easily be implemented in any reservoir simulation software and provide superior accuracy and performance for saturated oil viscosity of Iranian oil reservoirs than previously published correlations.

ACKNOWLEDGEMENTS

Research Institute of Petroleum Industry (RIPI) is acknowledged for providing the database and supporting this study. Finally, the primary author would like to thank his roommates, M. Nematzadeh, M. Seyed Kazemi, M. Lesani, H. Monjezi, and M. Aria. Without their patience and understanding, this may have never been written.

NOMENCLATURE

LSSVM : least square support vector machine
CSA : coupled simulated annealing
API : oil API gravity
P : pressure [psi]
P_b : bubble point pressure [psi]
R_s : solution gas-oil ratio [SCF/STB]
T : temperature [°F]
μ_o : oil viscosity [cp]
μ_{ob} : bubble point oil viscosity [cp]
μ_{od} : dead oil viscosity [cp]
E_i% : percent relative error
E_r% : average percent relative error
E_a% : average absolute percent relative error
RMSE : root mean square error
SD : standard deviation
R^2 : coefficient of determination
n : number of data points

REFERENCES

1. M. A. Al-Marhoun, *J. Pet. Sci. Eng.*, **42**, 209 (2004).
2. S. M. Farouq Ali, S., *J. Can. Pet. Technol.*, 35 (1996).
3. A. Elsharkawy and A. Alikhan, *Fuel*, **78**, 891 (1999).
4. Y. Gao and K. Li, *Fuel*, **95**, 431 (2012).
5. S. S. Ikiensikimama and O. Ogboja, *J. Pet. Sci. Eng.*, **69**, 214 (2009).
6. A. Naseri, M. Nikazar and S. A. Mousavi Dehghani, *J. Pet. Sci. Eng.*, **47**, 163 (2005).
7. A. Hemmati-Sarapardeh, M. Khishvand, A. Naseri and A. H. Mohammadi, *Chem. Eng. Sci.*, **90**, 53 (2013).
8. A. Hemmati-Sarapardeh, H. Hashemi Kiasari, N. Alizadeh, S. Mighani and A. Kamari, *Application of fast-SAGD in naturally fractured heavy oil reservoirs: A case study, in: The 18th Middle East Oil & Gas Show and Conference*, Bahrain (2013).
9. H. Hashemi-Kiasari, A. Hemmati-Sarapardeh, S. Mighani, A. H. Mohammadi and B. Sedaee-Sola, *Fuel*., **122**, 82 (2014).
10. A. Hemmati-Sarapardeh, S. Ayatollahi, M. H. Ghazanfari and M. Masihi, *J. Chem. Eng. Data*, **59**, 61 (2014).
11. F. Ahrabi, S. J. Ashcroft and R. B. Shearn, *Chem. Eng. Res. Design*, **65**, 63 (1987).
12. D.-H. Xu and A. K. Khurana, *A simple and efficient approach for improving the prediction of reservoir fluid viscosity, in: SPE Asia Pacific Oil and Gas Conference*, Society of Petroleum Engineers, Inc., Adelaide, Australia (1996).
13. J. E. Little, Kennedy, H. T, *Soc. Pet. Eng. J.*, **6**, 157 (1968).
14. A. Teja and P. Rice, *Ind. Eng. Chem. Fundam.*, **20**, 77 (1981).
15. S. E. Johnson, W. Y. Svrcek and A. K. Mehrotra, *Ind. Eng. Chem. Res.*, **26**, 2290 (1987).
16. S. E. Johnson, Svrcek, W. Y., *J. Can. Pet. Technol.*, **26**(5), 60 (1991).
17. O. S. Isehunwa, O. Olamigoke and A. A. Makinde, *A correlation to predict the viscosity of light crude oils, in: Nigeria Annual International Conference and Exhibition*, Society of Petroleum Engineers, Abuja, Nigeria (2006).
18. A. Hemmati-Sarapardeh, A. Shokrollahi, A. Tatar, F. Gharagheizi, A. H. Mohammadi and A. Naseri, *Fuel*, **116**, 39 (2014).
19. J.-N. Chew and C. A. Connally, *A viscosity correlation for gas-saturated crude oils* (1959).
20. H. D. Beggs and J. R. Robinson, *SPE J. Pet. Technol.*, **27**, 1140 (1975).
21. A. Al-Khafaji, G. Abdul-Majeed and S. Hassoon, *J. Pet. Res.*, 6 (1987).
22. G. E. J. Petrosky, *PVT Correlations for Gulf of Mexico Crude Oils*, MSC thesis, University of Sowthwestern Louisiana, Lufayette, Louisiana, USA (1990).
23. M. S. Hossain, C. Sarica, H.-Q. Zhang, L. Rhyne and K. L. Greenhill, *Assessment and development of heavy oil viscosity correlations, in: SPE/PS-CIM/CHOA International Thermal Operations and Heavy Oil Symposium*, Calgary, Alberta, Canada (2005).
24. D. F. Bergman and R. P. Sutton, *An update to viscosity correlations for gas-saturated crude oils, in: SPE Annual Technical Conference and Exhibition*, Society of Petroleum Engineers, Anaheim, California, USA (2007).
25. S. A. Khan, M. A. Al-Marhoun, S. O. Duffuaa and S. A. Abu-Khamsin, *Viscosity correlations for saudi arabian crude oils, in: Middle East Oil Show*, Society of Petroleum Engineers, Bahrain (1987).
26. R. Labedi, *J. Pet. Sci. Eng.*, **8**, 221 (1992).
27. J. A. K. Suykens and J. Vandewalle, *Neural Process. Lett.*, **9**, 293 (1999).

28. A. Eslamimanesh, F. Gharagheizi, M. Illbeigi, A. H. Mohammadi, A. Fazlali and D. Richon, *Fluid Phase Equilib.*, **316**, 34 (2012).
29. A. Fayazi, M. Arabloo, A. Shokrollahi, M. H. Zargari and M. H. Ghazanfari, *Ind. Eng. Chem. Res.*, **53**, 945 (2014).
30. A. Kamari, A. Khaksar-Manshad, F. Gharagheizi, A. H. Mohammadi and S. Ashoori, *Ind. Eng. Chem. Res.*, **52**, 15664 (2013).
31. A. Kamari, F. Gharagheizi, A. Bahadori, A. H. Mohammadi and S. Zendehboudi, *Fluid Phase Equilib*., **366**, 117 (2014).
32. H. Srinivas, K. Srinivasan and K. Umesh, *Adv. Theor. Appl. Mech.*, **3**, 159 (2010).
33. A. H. Mohammadi, A. Eslamimanesh, D. Richon, F. Gharagheizi, M. Yazdizadeh, J. Javanmardi, H. Hashemi, M. Zarifi and S. Babaee, *Ind. Eng. Chem. Res.*, **51**, 1062 (2011).
34. K. Pelckmans, J. A. K. Suykens, T. Van Gestel, J. De Brabanter, L. Lukas, B. Hamers, B. De Moor and J. Vandewalle, *LS-SVMlab: a matlab/c toolbox for least squares support vector machines*, Tutorial, KULeuven-ESAT, Leuven, Belgium (2002).
35. A. Eslamimanesh, F. Gharagheizi, A. H. Mohammadi and D. Richon, *J. Chem. Eng. Data*, **56**, 3775 (2011).
36. H. Liu, X. Yao, R. Zhang, M. Liu, Z. Hu and B. Fan, *J. Phys. Chem. B*, **109**, 20565 (2005).
37. A. Hemmati-Sarapardeh, R. Alipour-Yeganeh-Marand, A. Naseri, A. Safiabadi, F. Gharagheizi, P. Ilani-Kashkouli and A. H. Mohammadi, *Fluid Phase Equilib.*, **354**, 177 (2013).
38. A. Shokrollahi, M. Arabloo, F. Gharagheizi and A. H. Mohammadi, *Fuel*, **112**, 375 (2014).
39. S. R. Taghanaki, M. Arabloo, A. Chamkalani, M. Amani, M. H. Zargari and M. R. Adelzadeh, *Fluid Phase Equilib.*, **346**, 25 (2013).
40. M. M. Atiqullah and S. Rao, *Microelectronics Reliability*, **33**, 1303 (1993).
41. V. Fabian, *Computers & Mathematics with Applications*, **33**, 81 (1997).
42. A. Vasan and K. S. Raju, *Applied Soft Computing*, **9**, 274 (2009).
43. A. Kamari, A. Hemmati-Sarapardeh, S.-M. Mirabbasi, M. Nikookar and A. H. Mohammadi, *Fuel Process. Technol.*, **116**, 209 (2013).
44. J. A. K. Suykens, J. Vandewalle and D. E. M. Bart, *Int. J. Bifurcation and Chaos*, **11**, 2133 (2001).
45. S. Xavier-de-Souza, J. A. K. Suykens, J. Vandewalle and D. Bollé, *Coupled simulated annealing, Systems, Man, and Cybernetics*, Part B: Cybernetics, IEEE Transactions on, **40**, 320 (2010).
46. G. Koch, *Discovering multi-core: Extending the benefits of Moore's law*, Technology, 1 (2005).
47. A. Chamkalani, M. Amani, M. A. Kiani and R. Chamkalani, *Fluid Phase Equilib.*, **339**, 72 (2013).
48. M. Arabloo, M.-A. Amooie, A. Hemmati-Sarapardeh, M.-H. Ghazanfari and A. H. Mohammadi, *Fluid Phase Equilib.*, **363**, 121 (2014).
49. F. Gharagheizi and R. F. Alamdari, *A Molecular-Based Model for Prediction of Solubility of C60 Fullerene in Various Solvents, Fullerenes, Nanotubes, and Carbon Nonstructures*, **16**, 40 (2008).
50. J. Chew and C. Connally, *Trans. AIME*, **216**, 23 (1959).
51. H. Beggs and J. Robinson, *J. Pet. Technol.*, **27**, 1140 (1975).
52. A. Al-Khafaji, G. Abdul-Majeed and S. Hassoon, *J. Pet. Res.*, **6**, 1 (1987).
53. G. E. J. Petrosky, *PVT correlations for gulf of mexico crude oils*, MSC Thesis, University of Sowthwestern Louisiana, Lufayette, Louisiana, USA (1990).
54. M. S. Hossain, C. Sarica, H. Q. Zhang, L. Rhyne and K. Greenhill, *Assessment and development of heavy oil viscosity correlations, in: SPE International Thermal Operations and Heavy Oil Symposium*, Calgary, Canada (2005).
55. G. H. Abdul-Majeed, K. K. Clark and N. H. Salman, *J. Can. Pet. Technol.*, 29 (1990).
56. R. A. Almehaideb, *Improved PVT correlations for UAE crude oils, in: Middle East Oil Show and Conference*, Bahrain (1997).
57. B. Dindoruk and P. Christman, *PVT properties and viscosity correlations for Gulf of Mexico oils, in: SPE ATCE in New Orleans*, LA (2001).
58. T. Kartoatmodjo and Z. Schmidt, *Oil Gas J.*, **92**, 51 (1994).
59. S. Khan, M. Al-Marhoun, S. Duffuaa and S. Abu-Khamsin, *Viscosity correlations for Saudi Arabian crude oils, in: SPE Middle East Oil Show*, Manama, Bahrain (1987).
60. H. Orbey and S. I. Sandler, *Can. J. Chem. Eng.*, **71**, 437 (1993).
61. R. Sutton and D. Bergman, *Undersaturated Oil Viscosity Correlation for Adverse Conditions* (2006).
62. M. Vazquez and H. D. Beggs, *SPE J. Pet. Technol.*, **32**, 968 (1980).
63. Bergman, R. P. Sutton, *An update to viscosity correlations for gas-saturated crude oils, in: SPE Annual Technical Conference and Exhibition*, Society of Petroleum Engineers, Anaheim, California, USA (2007).